IEEE Access
Multidisciplinary | Rapid Review | Open Access Journal

SPECIAL SECTION ON RECONFIGURABLE INTELLIGENT SURFACE AIDED COMMUNICATIONS FOR 6G AND BEYOND

Received September 12, 2021, accepted October 6, 2021, date of publication October 11, 2021, date of current version October 19, 2021.

Digital Object Identifier 10.1109/ACCESS.2021.3119268

Aerial Reconfigurable Intelligent Surface-Enabled URLLC UAV Systems

YIJIU LI[1], CHENG YIN[1], TAN DO-DUY[2], ANTONINO MASARACCHIA[1], AND TRUNG Q. DUONG[1], (Senior Member, IEEE)

[1]School of Electronics, Electrical Engineering and Computer Science, Queen's University Belfast, Belfast BT3 9DT, U.K.
[2]Department of Computer and Communication Engineering, HCMC University of Technology and Education, Ho Chi Minh City 70000, Vietnam

Corresponding author: Trung Q. Duong (trung.q.duong@qub.ac.uk)

This work was supported in part by U.K. Royal Academy of Engineering (RAEng) under the RAEng Research Chair and Senior Research Fellowship Scheme Grant RCSRF2021\11\41, in part by the Engineering and Physical Sciences Research Council (EPSRC) under Grant EP/P019374/1, and in part by the EPSRC Impact Acceleration Accounts (IAA) Award.

ABSTRACT In this paper, we propose an aerial reconfigurable intelligent surface (RIS) system to support the stringent constraints of ultra-reliable low latency communication (URLLC). Specifically, unmanned aerial vehicles (UAVs) employed onboard RIS panels can act as repeaters to reflect the signal from macro base station (MBS) to all users in the networks. To overcome the dense networks' interference, we propose to use zero-forcing beamforming and time division multiplexing access (TDMA) scheme where each UAV can serve a number of users in its own cluster. We formulate a optimisation framework in terms of UAVs' deployment, power allocation at MBS, phase-shift of RIS, and blocklength of URLLC. Due to highly nonconvex and complex optimisation problem, we first consider to use a deep neural network (DNN) to solve the optimal UAVs' deployment. Then, the optimal resource allocation is proposed to provide the maximal reliability of the considered system with respect to the users' fairness. From the representative numerical results, our proposed scheme is shown to superior to other benchmarks which exhibits the positive impact of aerial RIS in supporting stringent demands of URLLC.

INDEX TERMS Ultra-reliable low-latency communications (URLLC), reconfigurable intelligent surface (RIS), unmanned aerial vehicle (UAV).

I. INTRODUCTION

Unmanned aerial vehicles (UAVs) have been widely applied in wireless communication systems as an efficient means to extend wireless coverage due to their flexible configuration and mobility nature [1], [2]. Specifically, UAVs play an important role when blockages exist between the base station (BS) and the user equipment (UE). UAVs are a brand-new technology used for surveillance, military, and even remote sensing [3]. According to previous studies, UAV-based communication networks possess outstanding ability to expand the transmit signal's coverage and improve transmission efficiency.

Reconfigurable intelligent surface (RIS) has been considered as a new technique for 6G networks. This technology is now under the spotlight because it can support energy-effective and cost-saving high data rate communication by using passive reflections [4]. RIS is an integrated panel that consists of passive reflecting elements [5] under the control of intelligent controllers and reflecting received signals toward the expected destinations. The intelligent controllers can help RIS to adapt the environment propagation, therefore, the received signals are enhanced, and the interference can be mitigated.

As a result, RIS-UAV systems have attracted much attention because of their abilities to enhance system performance [4], [6]. In [4], RIS is employed to support simultaneous wireless information and power transmission. RIS can also be employed at the cell boundary, creating a controlled propagation environment that improves user performance at the cell edge [6]. The authors formulate the weighted sum rate (WSR) maximisation problem, which is subject to the phase shift with unit modulus constraints while meeting the energy harvesting requirements. In [7], the authors analyse the performance of an integrated RIS-UAV relaying system, where the RIS is used to provide additional degrees of freedom, combined with UAVs, to improve the transmission quality between ground nodes. RIS carried by UAV approach

The associate editor coordinating the review of this manuscript and approving it for publication was Cunhua Pan.

has been proven to improve the performance of the system significantly in nonorthogonal multiple access (NOMA) [8], orthogonal frequency division multiple access (OFDMA) [9] and free-space optical (FSO) communication system [10]. The capacity and signal gain after applying the RIS-UAV system has been studied in [11], [12]. In [11], the RIS can be equipped with UAVs to apply certain phase shifts of the incident waves before it is reflected to the receiving UAV. It can also be deployed on building walls to reflect radio waves towards specific UAVs in order to improve their received signal gain and enhance the performance of UAVs cellular communications [13]. To avoid service starvation of cell-edge UEs and meet the QoS requirements, RIS is deployed on UAVs in [14]. By optimising the phase shifts matrix of RIS, the authors maximize the total energy efficiency (EE) of the system. With RIS's ability to improve the symbol error rate (SER), RIS-assisted UAV communications' capacity has been upgraded to ten times compared with traditional UAV communication systems [12]. In [15], the authors investigate a RIS-UAV radio system. The UAV is used to help the RIS reflect its own signal to the base station, while the RIS can enhance the UAV's transmission through passive beamforming. A novel secure RIS-assisted UAV system is proposed in [16]. Joint beamforming vector, trajectory and phase shift optimisation algorithm has been proposed in [17] to maximize the received signal at the ground users in the communication system. The post-disaster rescue by using the UAV carried with RIS has been studied in [18], and this research is meaningful for unforeseen natural disasters.

To meet the high demands of reliability and availability for new generation cellular networks, ultra-reliable and low-latency communications (URLLC) have been recognised as one of the major novel applications. This technique efficiently assists the critical mission communications in industrial automation [19], [20], disaster communications, environment monitoring and healthcare in terms of very low latency (from 1ms to few milliseconds) and ultra-high reliability (above 99.999%) [21]. To achieve such requirements, short packets transmissions are used to ensure the certain quality of service (QoS).

By combining the advantages of UAV and URLLC, the system eminently enhances its reliability and flexibility. UAVs' transmission that ensures the QoS requirements and URLLC rules has been investigated in [22], [23]. A logical UAV network has been created to accommodate multiple service requirements concurrently instead of satisfying separate network solutions for each type of service [22]. This network satisfies URLLC requirements for UAV control and non-payload signal transmission. In [24], the performance of cognitive UAV-URLLCs based on NOMA and massive machine-type communication (mMTC) services has been analysed. Optimisation method is frequently used in UAV assisted URLLC system research to meet service quality rules [23], [25]. Subject to the URLLC requirement, the block-length allocation and the UAV's location have been jointly optimised to minimise the decoding error probability [23]. In the UAV system, parameters have been optimised to maximize power efficiency in [25].

The combination of the UAV-RIS-URLLC system has been recognised as a completely new solution for future wireless networks. Although there is a huge potential of applying RIS with UAV in URLLC to cope with the significant increase in demand of stringent QoS services in 5G and beyond networks, the research in this direction is still in the early stage. To the best of our knowledge, only one published research utilises all advantages of RIS, UAV and URLLC [26]. The authors optimised the RIS passive beamforming antenna elements, the UAV's position and block-length to minimise the total decoding error rate. However, the RIS is deployed on buildings in [26] and the blocking effect still exists. To fill this gap, in our study, we propose a system with RIS carried by UAV, thus improving the flexibility of RIS. With the high demand of today's wireless communications, URLLC is crucial for industrial automation, the healthcare industry, vehicle safety and such scenarios. However, due to the complicated propagation environment, it is very challenging to meet the QoS requirements. The combination of UAV-URLLC can be considered as a good solution to this shortcoming. With the coverage extension provided by UAV, the whole system is more flexible and perform better in wireless communication scenarios. Moreover, UAVs are generally more cost-effective and more likely to establish line-of-sight (LoS) transmission links, which enhance communication performance. By cleverly turning the signal reflection low-cost passive reflective elements, the involvement of RIS enables the RIS-UAV-assisted URLLC system with even superior system performance. The main contributions of our paper include the following

- We propose an aerial RIS-assisted URLLC system where UAVs carry RIS panels to reflect the signal from main base station to far-end users. With this strategy, the stringent QoS requirements with very high reliability and very low latency of URLLC can be satisfied.
- We formulate a joint optimisation framework with respect to deployment of UAVs, the power allocation at base station, the phase shift of RIS, and the blocklength of URLLC to minimise the worst-case decoding error probability by taking into account the fairness of large-scale networks.
- To efficient solve the highly complex optimisation problem, we first propose a three-step deep neural network (DNN) framework including: i) training and testing, ii) building model, and iii) evaluating the solution. We demonstrate that the DNN model can predict the optimal locations of UAVs precisely and more rapidly compared to the conventional optimisation approach.
- We then solve the optimal resource allocation in terms of the phase-shift, power, and blocklength to optimise the minimum error decoding probability with respect to the ultra-reliability requirement. Our proposed optimisation algorithm outperforms the conventional

approaches which highlight the advantage of employing RIS onboard UAV to support URLLC.

The remainder of the paper is organised as follows. After the Introduction section, the system and channel models of RIS-UAV-assisted URLLC is presented in Section II. Specifically, in this section, we discuss the background of URLLC communications with less-than Shannon's achievable rate. Then, the UAV channel model, the transmission and beamforming design are also presented. The optimisation problem of the considered networks has been formulated in Section III. The optimal UAVs' deployment with DNN is introduced in Section IV. Then, the detailed solutions to solve the decoding error probability optimisation are provided in Section V. To illustrate the effectiveness of our optimisation framework, the simulation results are shown in Section VI. Finally, the conclusions are highlighted in Section VII.

II. RIS-UAV-ASSISTED URLLC SYSTEM MODEL

A. SYSTEM MODEL

We consider a URLLC system where a macro base station (MBS) serves a large number of users (UEs) with stringent QoS constrains, e.g., very low error probability and near-zero latency. Due to the severe shadowing and high pathloss effect, we employ a squadron of drones, a.k.a. UAVs, with RIS on-board to extend the network coverage. In the considered system, the MBS is equipped with a MIMO array with N transmit antennas to communicate with multiple UAVs for extending network coverage. The UAVs are used as small-cell flying base stations with RIS supporting very high URLLC communications. All UAVs can be connected to the cloud via a fog computing node aiming at expanding the coverage of reliable wireless networks.

Because of large-scale heterogeneous networks, the number of UEs may be very high, even greater than the number of transmit antenna at MBS, which leads to the loss of MIMO benefits. In addition, with high chances of line-of-sight (LOS) propagation of air-to-ground channel from UAVs, the inter-cell interferences can become a dominant factor to the degradation of network performance. To overcome these problems, we apply the TDMA transmission scheme by using M timeslots for M RIS-UAV clustering.

There are M RIS-UAVs working as relay nodes, denoted as a set of $\mathcal{M} = \{1, \ldots, M\}$ to serve K set of UEs $\mathcal{K} = \{1, \ldots, K\}$. The mth RIS-UAV will serve K_m UEs in its cluster by using UAV integrated RIS platform as shown in Fig. 1. All UEs are equipped with a single antenna and randomly distributed in the entire network.

B. ACHIEVABLE RATE AND DECODING ERROR PROBABILITY IN URLLC REGIME

In this subsection, we provide the overview of URLLC concept with the achievable rate of URLLC system (finite blocklength) under TDMA transmission scheme. Different from Shannon's capacity, for short blocklength communications, the coding rate r of the UE at a finite blocklength (b_m) in cluster m can be approximated as [27]:

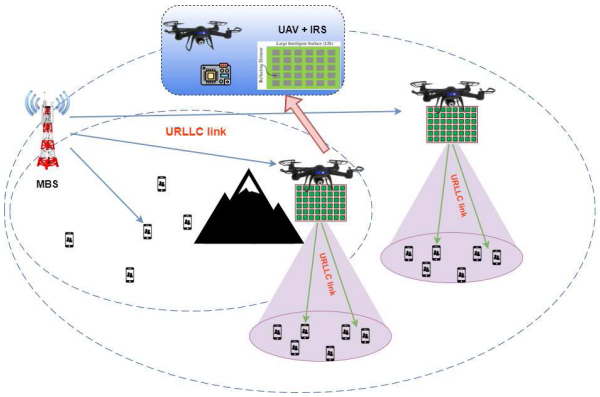

FIGURE 1. A model of URLLC-enabled UAV systems with RIS.

$$r \approx \log_2\left[1+\gamma(p_m)\right] - \sqrt{\frac{V(p_m)}{b_m}}\frac{Q^{-1}(\varepsilon)}{\ln 2} \tag{1}$$

where p_m is the transmit power from the MBS for the mth clustter, $\gamma(p)$ is the signal-to-noise ratio (SNR) at the receiver, $\varepsilon(p)$ is the decoding error probability, Q^{-1} is the inverse function of $Q(x) = \frac{1}{\sqrt{2\pi}}\int_x^\infty \exp^{\left(\frac{-t^2}{2}\right)} dt$, called the Q-function, and V given by $V(p) = 1 - [1+\gamma(p)]^{-2}$. From (1), the decoding error probability can be presented as follows:

$$\varepsilon = Q\left[f\left(\gamma, b_m, p_m, D\right)\right], \tag{2}$$

where

$$f\left(\gamma, b_m, p_m, D\right) = \ln 2\sqrt{\frac{b_m}{V(p_m)}}\left\{\log_2\left[1+\gamma(p_m)\right] - \frac{D}{b_m}\right\} \tag{3}$$

and D is the size of the transmitted packet.

C. AERIAL RIS-ASSISTED COMMUNICATION MODELS

Without loss of generality, we define the locations of the MBS, the RIS-UAVs, and of all UEs as $q_0 = (x_0, y_0, Z_0)$, $q_m = (x_m, y_m, Z_m)$, $m \in \mathcal{M}$ and $q_k = (x_k, y_k, 0)$, $k \in \mathcal{K}_U$, respectively. The antenna height of the BS and the UAV altitude are respectively denoted as Z_0 and Z_m.

With high probability of the LoS propagation in air-to-air (ATA) links, the path loss of the link between the MBS and m-th RIS-UAV follows the free-space path loss model as [1], [28]

$$\beta_{0,m}^{ata} = \beta_0 r_{0,m}^{-2}, \quad m = 1, \ldots, M, \tag{4}$$

where β_0 is the channel's power gain at reference distance d_0 and $d_{0,m}$ is the distance between the MBS and the mth RIS-UAV given by $r_{0,m} = \sqrt{d_{0,m}^2 + (Z_0 - Z_m)^2}$, where $d_{0,m} = \sqrt{(x_0 - x_m)^2 + (y_0 - y_m)^2}$.

The air-to-ground (ATG) channels between UAVs and UEs are also dominant by LoS propagation but they are more

complex due to the effects of propagation attenuation by shadowing and blockage geometry [29]. As such, the path loss of the link between the m-th RIS-UAV and the (m, k)-th UE can be written as

$$\begin{aligned}\beta_{m,k} &= PL_{m,k} + \eta^{LoS} P_{m,k}^{LoS} + \eta^{NLoS} P_{m,k}^{NLoS} \\ &= 10\alpha \log\left(\sqrt{d_{m,k}^2 + Z_m^2}\right) + AP_{m,k}^{LoS} + B, \end{aligned} \tag{5}$$

where η^{LoS} and η^{NLoS} are the average additional losses for LoS and NLoS, respectively. $A = \eta^{LoS} - \eta^{NLoS}$ and $B = 10\alpha \log\left(\frac{4\pi f_c R_{m,k}}{c}\right) + \eta_{NLoS}$. The distance path loss is given by

$$PL_{m,k} = 10 \log\left(\frac{4\pi f_c R_{m,k}}{c}\right)^{\alpha}, \tag{6}$$

where f_c is carrier frequency (Hz), c is the speed of light (m/s), $\alpha \geq 2$ is the path loss exponent. The probability of LoS and NLoS is shown as

$$P_{m,k}^{LoS} = \frac{1}{1 + a \exp\left[-b\left(\arctan\left(\frac{Z_m}{d_{m,k}}\right) - a\right)\right]} \tag{7}$$

$$P_{m,k}^{NLoS} = 1 - P_{m,k}^{LoS}, \tag{8}$$

where the constants a and b depend on the specific arrangement of the environment.

Moreover, for the small-scale fading, the channel coefficients of the channels from MBS to m-th UAV-RIS and from the m-th UAV-RIS to the (m, k)-th UE are denoted by $\boldsymbol{g}_{0,m} \in \mathbb{C}^{R\times N}$ and $\boldsymbol{h}_{m,k}^H \in \mathbb{C}^{1\times R}$, respectively. Here, these small-scale fading coefficients are assumed to be independent and identically distributed (i.i.d.) random variables with zero mean and unit variance, where the $(\cdot)^H$ represents the conjugate transpose operation, and R is the number of elements of the RIS. Next, we denote $\boldsymbol{G}_{0,m} \in \mathbb{C}^{R\times N}$ and $\boldsymbol{H}_{m,k}^H \in \mathbb{C}^{1\times R}$ as the channel matrix from the MBS to m-th RIS-UAV and from the m-th RIS-UAV to the (m, k)-th UE in the m-th cluster, respectively. Hence, the cascaded channel matrix of the link from the MBS to the (m, k)-th UE via the m-th UAV-RIS, named $\boldsymbol{F}_{m,k} \in \mathbb{C}^{1\times N}$, can be expressed as

$$\boldsymbol{F}_{m,k} = \boldsymbol{H}_{m,k}^H \boldsymbol{\Phi}_m \boldsymbol{G}_{0,m} \tag{9}$$

where $\boldsymbol{H}_{m,k}^H = \sqrt{\beta_{m,k}}\boldsymbol{h}_{m,k}^H$; $\boldsymbol{G}_{0,m} = \sqrt{\beta_{0,m}}\boldsymbol{g}_{0,m}$, and $\boldsymbol{\Phi}_m = \text{diag}\left[\eta_{1m}e^{j\theta_{1m}}, \eta_{2m}e^{j\theta_{2m}}, \ldots, \eta_{Rm}e^{j\theta_{Rm}}\right]$ is the diagonal matrix of size $R \times R$ at the m-th RIS-UAV with $\eta_{rm} \in [0, 1]$; $\theta_r \in [0, 2\pi]$ represent reflection coefficient and the phase shift value of the r-th element at the RIS.

D. TRANSMISSION AND BEAMFORMING SCHEMES

As shown in Fig. 1, the RIS panel deployed on UAV reflects the signal from the MBS to M groups of UEs in the UAVs's coverage. The received signal at the (m, k)th UE of the m-th cluster (m-th RIS-UAV) are written as[1]

$$\begin{aligned} y_{m,k} = &\underbrace{\sqrt{P_0}\boldsymbol{F}_{m,k}\boldsymbol{w}_{m,k}s_{m,k}}_{\text{desired signal}} \\ &+ \underbrace{\sqrt{P_0}\sum_{i=1,i\neq k}^{K_m}\boldsymbol{F}_{m,k}\boldsymbol{w}_{m,i}s_{m,i}}_{\text{intra-cell interference}} + n_{m,k}, \end{aligned} \tag{10}$$

where P_0 is the transmit power at the MBS, $\boldsymbol{w}_{m,k} \in \mathbb{C}^{N\times 1}$ are transmit beamforming vector of the MBS, and $s_{m,k}$ is information transmitted by the MBS with $||s_{m,k}||^2 \leq 1$, $n_{m,k} \sim \mathcal{CN}(0, \sigma_{m,k}^2)$ is the AWGN at the (m, k)-th UE.

1) MRT APPROACH

In this subsection, we apply MRT for MIMO beamforming design with the beamforming vector as

$$\boldsymbol{w}_{m,k} = \sqrt{p_{m,k}}\frac{\left(\boldsymbol{F}_{m,k}^H\right)^*}{\|\boldsymbol{F}_{m,k}^H\|}, \forall m, \tag{11}$$

where $0 < p_{m,k} < 1$ is the power coefficient control of the MBS for k-th UE in m-th RIS-UAV. Then, the decoding error probability of the (m, k)th UE for downlink transmission with TDMA scheme can be presented as

$$\varepsilon_{m,k} = Q\left[f\left(\gamma_{m,k}, b_m, p_{m,k}, D\right)\right], \tag{12}$$

where

$$\begin{aligned} f\left(\gamma_{m,k}, b_m, p_{m,k}, D\right) = &\ln\left(2\sqrt{\frac{b_m}{V(p_{m,k})}}\right) \\ &\times \left\{\log_2\left[1 + \gamma_{m,k}(p_{m,k})\right] - \frac{D}{b_m}\right\}, \end{aligned} \tag{13}$$

and

$$\gamma_{m,k}(p_{m,k}) = \frac{P_0|\boldsymbol{F}_{m,k}\boldsymbol{w}_{m,k}|^2}{\sum_{i\in\mathcal{K}_m, i\neq k} P_0|\boldsymbol{F}_{m,k}\boldsymbol{w}_{m,i}|^2 + \sigma_{m,k}^2} \tag{14}$$

2) ZF APPROACH

In this subsection, we first seek the beamforming vector $\bar{\boldsymbol{w}}_m = [\bar{\boldsymbol{w}}_{m,1}, \ldots, \bar{\boldsymbol{w}}_{m,K_m}] \in \mathbb{C}^{N\times K_m}$ in the class of zero-forcing (ZF) as follows. Let us denote

$$\bar{\boldsymbol{W}} = [\bar{\boldsymbol{w}}_1, \ldots, \bar{\boldsymbol{w}}_M] = \boldsymbol{F}^H(\boldsymbol{F}\boldsymbol{F}^H)^{-1}, \tag{15}$$

where $\boldsymbol{F} = [\boldsymbol{F}_1, \ldots, \boldsymbol{F}_M]^T \in \mathbb{C}^{K\times N}$, $\boldsymbol{F}_m = [\boldsymbol{F}_{m,1}, \ldots, \boldsymbol{F}_{m,K_m}]^T \in \mathbb{C}^{K_m\times N}$. We normalize ZF beamforming vector as $\bar{\boldsymbol{w}}_{m,k}/\|\bar{\boldsymbol{w}}_{m,k}\|$, and seek $\boldsymbol{w}_{m,k}$ in the class of

$$\boldsymbol{w}_{m,k} = \sqrt{p_{m,k}}\frac{\bar{\boldsymbol{w}}_{m,k}}{\|\bar{\boldsymbol{w}}_{m,k}\|}, \forall m \tag{16}$$

where $0 < p_{m,k} < 1$ is the power coefficient control of the MBS for k-th UE in m-th UAV. Then, the decoding error probability of the (m, k)-th UE with ZF can be presented as

$$\varepsilon_{m,k} = Q\left[f\left(\gamma_{m,k}, b_m, p_{m,k}, D\right)\right], \tag{17}$$

[1]The inter-cell interference in (10) is removed by using TDMA transmission scheme.

where

$$f\left(\gamma_{m,k}, b_m, p_{m,k}, D\right) = \ln\left(2\sqrt{\frac{b_m}{V(p_{m,k})}}\right) \times \left\{\log_2\left(1+\gamma_{m,k}\right) - \frac{D}{b_m}\right\}, \quad (18)$$

and

$$\gamma_{m,k}(p_{m,k}) = \frac{P_0|\boldsymbol{F}_{m,k}\boldsymbol{w}_{m,k}|^2}{\sigma_{m,k}^2} \quad (19)$$

$$= \frac{P_0 p_{m,k}}{\sigma_{m,k}^2}\left|\frac{\boldsymbol{F}_{m,k}\bar{\boldsymbol{w}}_{m,k}}{\|\bar{\boldsymbol{w}}_{m,k}\|}\right|^2 \quad (20)$$

is the SNR at the UE with ZF beamforming.[2]

Since the decoding error probability with Q function is highly complex, it is profoundly difficult to solve the reliability optimisation directly with the original form. Therefore, we apply the linear approximation $\varepsilon \approx \mathbb{E}[E(\gamma)]$ [19], [20], [30], [31] as

$$E(\gamma) = \begin{cases} 1, & \gamma < \alpha \\ 1 - v\sqrt{b_m}\,(\gamma - \theta), & \alpha < \gamma < \beta \\ 0, & \gamma \geq \beta, \end{cases} \quad (21)$$

where $v = \frac{1}{2\pi\sqrt{2^{\frac{2D}{b_m}}-1}}$, $\theta = \frac{2D}{b_m} - 1$, $\alpha = \theta - \frac{1}{2v\sqrt{b_m}}$, $\beta = \theta + \frac{1}{2v\sqrt{b_m}}$. Then, by applying the above approximation, the decoding error probability can be evaluated as

$$\varepsilon \approx \int_0^\infty E(x) f_\gamma(x)\,dx = v\sqrt{b_m}\int_\alpha^\beta F_\gamma(x)\,dx. \quad (22)$$

From [31], the cumulative distribution function is defined as

$$F_\gamma(x) = 1 - \exp\left(-\frac{x}{\gamma}\right) \overset{\text{high SNR}}{\approx} \frac{x}{\gamma}. \quad (23)$$

Finally, combining (22) and (23) together, the point-to-point decoding error probability is written as

$$\varepsilon_{m,k} = \frac{1}{\gamma_{m,k}(p_{0,m})}\left(2^{\frac{D}{b_m}} - 1\right). \quad (24)$$

III. PROBLEM FORMULATION

Our target is to minimise decoding error probability under blocklength and power allocation optimisation for URLLC-enabled UAV system with RIS. Due to a highly complex structure of interference in the SNR formula of MRT beamforming, for the sake of simplicity, we only consider the case of ZF beamforming in this paper. As such, the corresponding decoding error probability minimisation problem for ZF approach is formulated as

$$\min_{\boldsymbol{p},\boldsymbol{b},\boldsymbol{q}k=1,\ldots,K_m} \max \varepsilon_{m,k}, \forall m \in \mathcal{M}, \forall k \in \mathcal{K}, \quad (25a)$$

$$\text{s.t.} \sum_{m=1}^{M} b_m \leq BL^{\max}, \forall m \in \mathcal{M}, \quad (25b)$$

$$\sum_{m=1}^{M}\sum_{k=1}^{K_m} \frac{b_m p_{m,k}}{BL^{\max}} \leq 1, \forall m \in \mathcal{M} \quad (25c)$$

$$\sum_{m=1}^{M}\sum_{k\in\mathcal{K}_m} p_{m,k} \leq 1, \forall m \in \mathcal{M}, \quad (25d)$$

$$b_m \in \mathbb{Z}^+, \forall m \in \mathcal{M}, \quad (25e)$$

$$(m,k) \in \mathcal{K}_m, \forall m \in \mathcal{M}, \forall k \in \mathcal{K}_m \quad (25f)$$

$$K_m \in \mathbb{Z}^+, K_m \leq K_m^{max} \quad (25g)$$

where $BL^{\max}$ is maximum blocklength of the MBS. The constraints (25b) represent the latency requirement. The constraints (25c), and (25d) are the power requirement at the MBS. The constraint (25e) means the blockength is integer number. The constraints (25f), (25g) are the UAVs-UEs clustering problem.

In this paper, we divide the optimisation problem into the two subproblems. We first deal with the optimal UAVs deployment and then the optimal resource allocation for minimising the error probability.

IV. PROPOSED SOLUTION FOR UAV DEPLOYMENT

In this subsection, we address the problem of optimal UAV deployment before solving the decoding error probability optimisation problem. The UAV deployment procedure actually is a clustering problem to form a network of RIS-UAVs and UEs that satisfies the constraints (25f) and (25g). The objective of this clustering problem is to optimise the position of RIS-UAVs so that RIS-UAVs can serve as many UEs as possible in their coverage range. Based on this concept, we formulate an mixed (binary) integer programming problem for the RIS-UAVs deployment.

We consider the maximum coverage area of an RIS-UAV by defining a circular disc of radius $D_{m,cov}$. This value is calculated based on the altitude of the m-th RIS-UAV as follows

$$H_m = D_{m,cov}\tan(\theta), \forall m, \quad (26)$$

where θ is set to 42.44° [32]. Then the (m,k)-th UE belongs to the m-th cluster served by the m-th RIS-UAV if the Euclidean distance between the k-th UE and the m-th RIS-UAV ($d_{m,k}$) is lower or equal to the maximum coverage distance $D_{m,cov}^{max}$, which can be expressed as

$$d_{m,k} \leq D_{m,cov}^{max}\, k \in \mathcal{K}_m, \quad (27)$$

where $D_{m,cov}^{max} = H_m^{max}/\tan(\theta)$. We then introduce a binary variable $\phi_{m,k} = \{0, 1\}$ representing that the k-th UE and the m-th RIS-UAV belong to the same cluster m-th or not.

Finally, the clustering problem can be expressed as follows:

$$\max_{\boldsymbol{q},\boldsymbol{\phi}} \sum_{m=1}^{M}\sum_{k=1}^{K_m} \phi_{m,k} \quad (28a)$$

$$\text{s.t. } d_{m,k}^2 \leq (D_{m,cov}^{max})^2 + \lambda_m(1-\phi_{m,k}), \quad (28b)$$

$$\boldsymbol{q}_m \in [\boldsymbol{q}_m^{\min}, \boldsymbol{q}_m^{max}], \quad (28c)$$

[2]Compared with the MRT approach in (10), the intra-cell interference can be removed by using ZF beamformer.

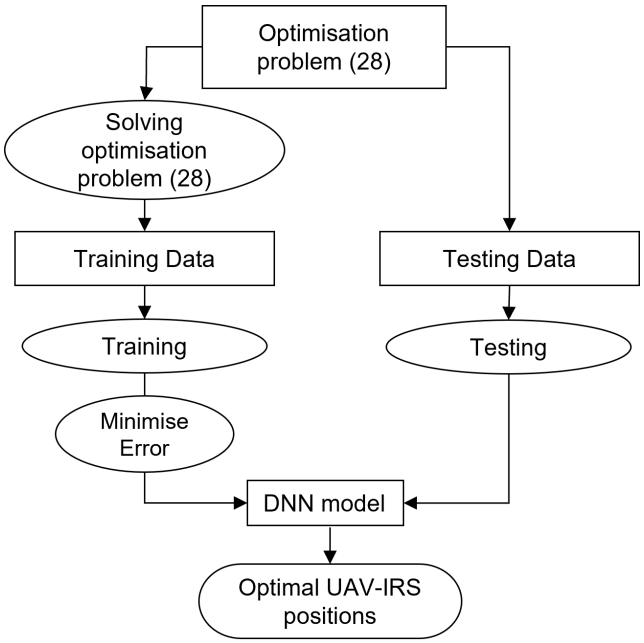

FIGURE 2. The diagram of proposed DNN-based RIS-UAVs deployment solution.

$$\phi_{m,k} \in \{0, 1\}, \tag{28d}$$

$$(25g), \tag{28e}$$

$$m \in \mathcal{M},\ k \in \mathcal{K}_m,$$

where λ_m is chosen as a specific corresponding value to maximize network coverage area of the m-th RIS-UAV (e.g., $\lambda_m > (D^{max}_{m,cov})^2$), $[\boldsymbol{q}^{\min}_m, \boldsymbol{q}^{max}_m]$ are the lower and upper bounds of the horizontal and vertical range of RIS-UAVs, respectively.

As we can observe that the problem (28) is a mixed-integer quadratic programming, which belongs to combinatorial (or discrete) optimisation problem. This kind of problem is often very difficult to solve in real-time. Although there are some well-known packages such as CVX, CVXPY can solve the problem by using appropriate solvers, solving this conventional problem takes time, especially in large-scale scenarios. Therefore, we follow the same approach as in [19], [33]–[35] by proposing a learning-aid solution using DNN to solve this problem rapidly.

Our proposed DNN-based solution for RIS-UAVs deployment is displayed as Fig. 2. In particular, this method includes three main steps: (i) formulating the optimisation problem, (ii) generating data for training and testing, (iii) building the DNN model and evaluating the solution. The problem formulation in the first step is fully discussed as above in this section and problem is finally presented as (28).

For the second step, we repeatedly solve the problem (28) to generate sufficiently large data for the training phase. Firstly, we create around 200 system model scenarios with random locations of RIS-UAVs and UEs. Then we implement a CVXPY function in Python for solving the problem (28) in order to obtain the optimal values of RIS-UAVs' location for all generated scenarios. After knowing these optimal location of RIS-UAVs, we save these value as the output of the DNN model that is designed as follows in the third step.

The last step is designing a DNN model for finding the optimal locations of RIS-UAVs rapidly. Our DNN model consists of three hidden layers with the size of 200, 80, 80 neurons, respectively. The neural network is fully connected, and uses "sigmoid" function for hidden layer, while the output layer is "linear" activation function to provide the predicted value of the RIS-UAVs' locations. The model is compiled by a gradient-based optimisation technique named RMSprop with the mean absolute error (MAE) metric. After that, we use the dataset created in the second step for training and creating the DNN model, which can predict the optimal locations exactly and rapidly compared to the conventional optimisation solution. The effectiveness of our DNN-based method is presented in Table 1 in the simulation results section.

V. PROPOSED SOLUTION FOR DECODING ERROR PROBABILITY OPTIMISATION

To solve the optimisation problem (25), we proposed an iterative algorithm, which is fully presented in Algorithm 1. The basic concept is that at the i-th iteration, we solve the problem (25) with fixed blocklength $b^{(i)}_m$ to find next optimal values of power $p^{(i+1)}_{m,k}$. Then we solve the problem (25) with these current optimal $p^{(i+1)}_{m,k}$ to find the next optimal values of the blocklength $b^{(i+1)}_m$. When we fix one variable and solve problem with the remain variable, the problem (25) is convex program, which can be solved directly with well-known tools such as CVX, CVXPY. The procedure is repeated until convergence or reaches the maximum number of iterations I^{iter}_{max}. The initial values of blocklength $b^{(0)}_m$ are chosen randomly that satisfy the constraints (25b), (25e).

VI. SIMULATION RESULTS

In this section, the performance of the considered network is evaluated to demonstrate the effectiveness of the proposed URLLC RIS-UAV communications. For the optimal UAVs deployment, we use the CVXPY version 1.0.21 in Python [36] to implement the DNN. The system parameters of simulations results are set up as follows. The MBS area is a circle coverage with a radius of 500m whereas the extended area of the MBS is covered with a radius up to 2000m. We assume that the MBS is located at $(0, 0, 30)$ while UEs are randomly distributed in the network. The limited altitude of the UAVs (H^{min}, H^{max}) is $(5, 20)$m. The AWGN spectral density is $\sigma^2 = -130$ dBm/Hz. Unless otherwise stated, other parameters of the channel model are defined as in [28], [32], [37]. The maximum blocklength of the MBS is set at $BL^{max} = 200$ (symbols) [38], [39].

A. EFFECTIVENESS OF DNN-BASED RIS-UAVs DEPLOYMENT

To demonstrate the performance of the DNN-based approach in RIS-UAVs deployment over the conventional optimisation

Algorithm 1 Proposed Algorithm to Solve (25)

Input: The number of RIS-UAV (M), UEs (K).
The power budget of the MBS (P_{max}).
The blocklength budget of MBS (M_{max}).
The maximum number of iterations is set to I_{max}^{iter}.
AND
Set i=0, initial fixed block-length $b_m^{*(0)}$

Repeat
  Find the optimal transmit power ($p_{m,k}^{*(i+1)}$)
    Solve the optimisation problem (25) with fixed blocklength ($b_m^{*(i+1)}$)
    Obtain the current optimal power ($p_{mk}^{*(i+1)}$)
  Find optimal blocklength ($b_m^{*(i+1)}$)
    Solve the optimisation problem (25) with fixed power values ($p_{kn}^{*(i+1)}$)
    Obtain the current blocklength ($b_m^{*(i+1)}$)
  Set $i = i + 1$,
Until
    Convergence, or the iteration number reaches I_{max}^{iter}
Calculate overall error

Output: the optimal value of worst-case decoding error probability

TABLE 1. The comparison Conv. OPT versus DNN-based approach in term of execution time among different scenarios.

Scenarios	Conv. OPT	DNN	Accuracy
M=2, Km = 10	0.13s	0.04s	91.6%
M=3, Km = 20	0.5s	0.04s	89.7%
M=4, Km = 30	1.6s	0.04s	96.7%

approach, we compare the execution time of the DNN-based approach (DNN) and the conventional optimisation solution (Conv. OPT). Table 1 provides the execution time in RIS-UAVs positioning of two methods among different scenarios. As we can observe from the table, the DNN-based approach significantly outperforms the Conv. OPT in term of execution time, especially in large-scale scenarios. Interestingly, when the number of RIS-UAVs and UEs increases, the execution time of DNN-based method stays at the same level ($0.04s$), while that steadily rises in the Conv. OPT (from 0.13s to 1.6s).

B. DECODING ERROR PROBABILITY VERSUS THE NUMBER OF ELEMENTS OF RIS

Table 2 gives information about the effectiveness of RIS-UAVs in increasing reliability of URLLC systems. In particular, the table compares the decoding error probability among different number of RIS's elements with the transmit power range of $P_0 = [40, 50]$ dBm. Obviously, the more elements the RIS-UAVs have, the more reliability system can achieve. Particularly, when the support of RIS is minimal (e.g., $R = 1$), the decoding error probability is up to 10^{-3} at $P_0 = 50$ dBm, which does not satisfy the URLLC requirements. It is important to note that for many importance applications such as smart grid, e-health, intelligent transport system (ITS), V2V, AR, the minimum required reliability is 99.999% [21]. Clearly from this table, we can see that the employment of RIS has played an important role in support the aforementioned URLLC applications. Differently, in RIS-aided scenarios, the reliability reaches to $1-10^{-6}$ that meet stringent demand for many URLLC-based applications.

TABLE 2. The effectiveness of RIS-UAV enabling URLLC systems.

P0	40 dBm	42 dBm	44 dBm	46 dBm	48 dBm	50 dBm
RIS R = 1	1.45E-02	9.13E-03	5.76E-03	3.63E-03	2.29E-03	1.45E-03
RIS R = 15	7.09E-05	4.47E-05	3.10E-05	2.04E-05	1.36E-05	8.55E-06
RIS R = 20	6.16E-05	3.88E-05	2.73E-05	2.33E-05	1.38E-05	9.24E-06
RIS R = 30	4.03E-05	2.84E-05	1.97E-05	1.24E-05	8.27E-06	5.62E-06

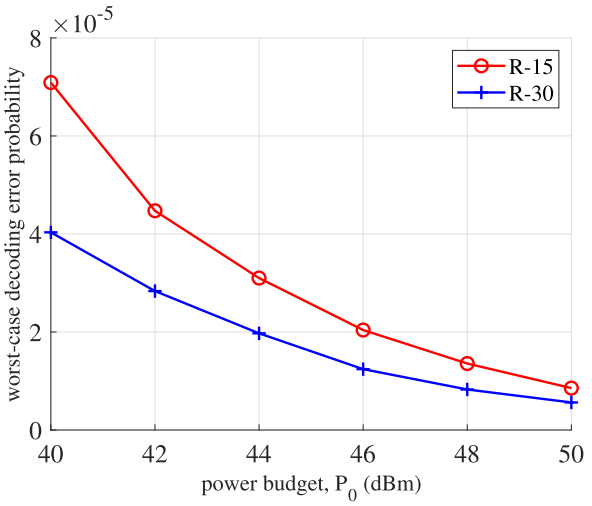

FIGURE 3. The comparison of worst-case decoding error probability among different number element of RIS in the scenarios of $M = 2$ RIS-UAV, $K = 6$ UEs.

Fig. 3 plots the worst-case decoding error probability of the scenarios of $M = 2$ RIS-UAVs and $K = 6$ UEs with different values of RIS's elements. As the figure shows, the RIS-UAV with 30 element is better than that with 15 elements in terms of improving the reliability of URLLC system.

C. DECODING ERROR PROBABILITY WITH OPTIMAL POWER ALLOCATION AND BLOCKLENGTH

To illustrate the effectiveness of the proposed iterative optimisation algorithm, we compare the optimal power allocation solution with the equal power allocation in reducing decoding error probability. Fig. 4 displays the performance of the proposed power allocation solution in improving the reliability. As we can observe from the figure, the optimal blocklength and power allocation is always better than the equal power allocation, especially when the power budget of the system is small.

Fig. 4 also compares the worse-case decoding error probability of UEs among different level of MBS's power budget in optimal blocklength and equal blocklength schemes. Obviously, the proposed optimal blocklength and power allocation solution effectively improves the reliability compared with the equal blocklength allocation.

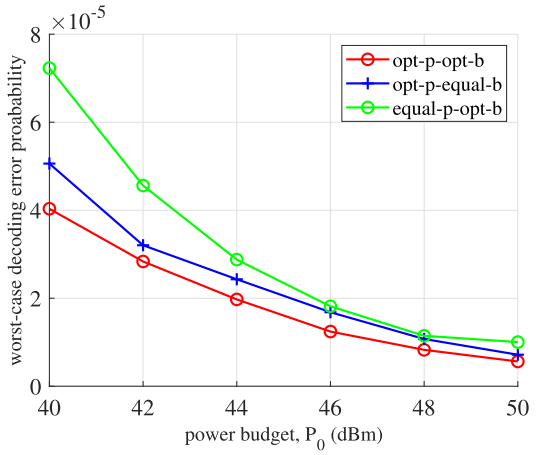

FIGURE 4. The comparison of worst-case decoding error probability among different power budget of the MBS in the scenarios of $M = 2$ RIS-UAV, $K = 6$ UEs, $R = 30$ elements: optimal power allocation versus equal power.

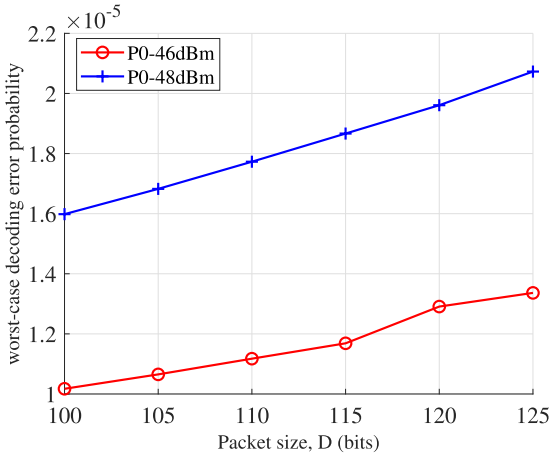

FIGURE 5. The comparison of worst-case decoding error probability among different packet size D (bits) in the scenarios of $M = 2$ RIS-UAV, $K = 6$ UEs, $R = 30$ elements.

D. DECODING ERROR PROBABILITY VERSUS PACKET SIZE

To demonstrate the impact of packet size (D) on the performance of URLLC-based communications, Fig. 5 compares the worst-case decoding error probability of UEs in the scenarios of $M = 2$ RIS-UAVs, $K = 6$ UEs, and $R = 30$ elements in two transmit budget level $P_0 = [46, 48]$ dBm with different number of the packet sizes [100, .., 125] bits. As expected, the smaller packet size is, the higher reliability the URLLC system can achieve.

E. DECODING ERROR PROBABILITY VERSUS NUMBER OF UEs

Fig. 6 compares the achieved reliability level of two model with the same number of RIS-UAVs ($M = 2$) and different number of served UEs ($K_m = [3, 6]$). As we can observe from the figure, with the same number of RIS-UAVs, the more number of UEs the clusters have, the more error can occur

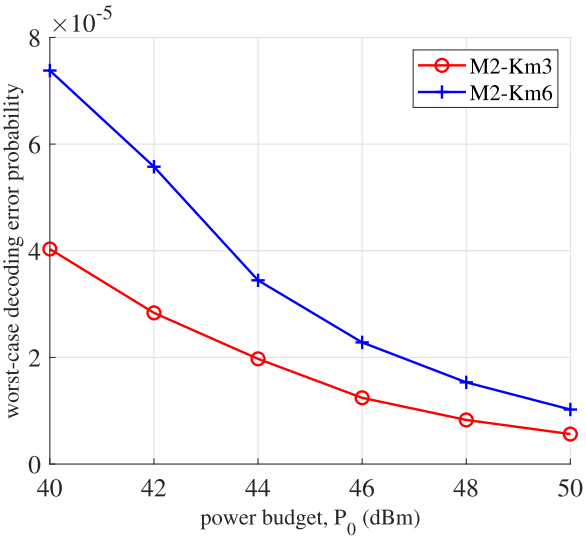

FIGURE 6. The comparison of worst-case decoding error probability among different number of UEs with equal RIS-UAV ($M = 2$), $R = 30$ elements.

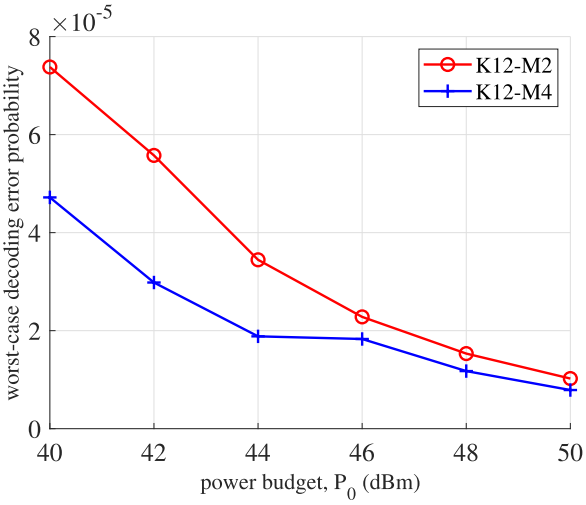

FIGURE 7. The comparison of worst-case decoding error probability among different number of RIS-UAV with equal number of UEs ($K = 12$), $R = 30$ elements.

during transmissions, especially in the system with limited power budget.

F. DECODING ERROR PROBABILITY VERSUS NUMBER OF RIS-UAV

To illustrate the impact of RIS on the performance of URLLC system, we compare the reliability of scenarios that have the same number of UEs and different number of RIS-UAVs. Fig. 7 plots the worst-case decoding error probability of two scenarios $K = 12, M = 2$ and $K = 12, M = 4$ among power budget of $P_0 = [40, 50]$ dBm. Obviously, with the same number of UEs, the higher number of RIS-UAVs, the better reliability the system can offer.

VII. CONCLUSION

In this paper, to support various QoS's requirements of URLLC, we have proposed an aerial RIS-UAV system to

assist the direct communications between a MBS employed with ZF beamforming and UEs. To overcome the severe shadowing and pathloss, each UAV carrying an RIS panel onboard serves as many as UEs in its cluster. We have formulated the optimal resource allocations in terms of UAVs, MBS's power, RIS's phase-shift, and blocklength. Due to the extreme complex optimisation problem, we have separated the optimisation problem into two sub-problems. Firstly, the optimal UAVs' deployment can be solved using DNN frameworks with fasted execution time compared with conventional optimisation approach. Secondly, the optimisation algorithm to solve the minimum decoding error probability of the worst-case user has been proposed. We have demonstrated through the extensive numerical results that our proposed optimisation scheme outperforms other existing approach which reveals the importance of using RIS onboard UAV to support URLLC for the next generation of wireless networks.

ACKNOWLEDGMENT

The authors would like to thank Dang Van Huynh for his helpful discussion and suggestion.

REFERENCES

[1] M.-N. Nguyen, L. D. Nguyen, T. Q. Duong, and H. D. Tuan, "Real-time optimal resource allocation for embedded UAV communication systems," *IEEE Wireless Commun. Lett.*, vol. 8, no. 1, pp. 225–228, Feb. 2019.

[2] L. Nguyen, A. Kortun, and T. Duong, "An introduction of real-time embedded optimisation programming for UAV systems under disaster communication," *EAI Endorsed Trans. Ind. Netw. Intell. Syst.*, vol. 5, no. 17, Dec. 2018, Art. no. 156080.

[3] A. Thakare, E. Lee, A. Kumar, V. B. Nikam, and Y.-G. Kim, "PARBAC: Priority-attribute-based RBAC model for azure IoT cloud," *IEEE Internet Things J.*, vol. 7, no. 4, pp. 2890–2900, Apr. 2020.

[4] C. Pan, H. Ren, K. Wang, M. Elkashlan, A. Nallanathan, J. Wang, and L. Hanzo, "Intelligent reflecting surface aided MIMO broadcasting for simultaneous wireless information and power transfer," *IEEE J. Sel. Areas Commun.*, vol. 38, no. 8, pp. 1719–1734, Aug. 2020.

[5] H. Ren, K. Wang, and C. Pan, "Intelligent reflecting surface-aided URLLC in a factory automation scenario," 2021, *arXiv:2103.09323*. [Online]. Available: http://arxiv.org/abs/2103.09323

[6] C. Pan, H. Ren, K. Wang, W. Xu, M. Elkashlan, A. Nallanathan, and L. Hanzo, "Multicell MIMO communications relying on intelligent reflecting surfaces," *IEEE Trans. Wireless Commun.*, vol. 19, no. 8, pp. 5218–5233, Aug. 2020.

[7] T. Shafique, H. Tabassum, and E. Hossain, "Optimization of wireless relaying with flexible UAV-borne reflecting surfaces," *IEEE Trans. Commun.*, vol. 69, no. 1, pp. 309–325, Jan. 2021.

[8] S. Jiao, F. Fang, X. Zhou, and H. Zhang, "Joint beamforming and phase shift design in downlink UAV networks with IRS-assisted NOMA," *J. Commun. Inf. Netw.*, vol. 5, no. 2, pp. 138–149, Jun. 2020.

[9] Z. Wei, Y. Cai, Z. Sun, D. W. K. Ng, J. Yuan, M. Zhou, and L. Sun, "Sum-rate maximization for IRS-assisted UAV OFDMA communication systems," *IEEE Trans. Wireless Commun.*, vol. 20, no. 4, pp. 2530–2550, Apr. 2021.

[10] H. Jia, J. Zhong, M. N. Janardhanan, and G. Chen, "Ergodic capacity analysis for FSO communications with UAV-equipped IRS in the presence of pointing error," in *Proc. IEEE 20th Int. Conf. Commun. Technol. (ICCT)*, Oct. 2020, pp. 949–954.

[11] M. Al-Jarrah, E. Alsusa, A. Al-Dweik, and D. K. C. So, "Capacity analysis of IRS-based UAV communications with imperfect phase compensation," *IEEE Wireless Commun. Lett.*, vol. 10, no. 7, pp. 1479–1483, Jul. 2021.

[12] A. Mahmoud, S. Muhaidat, P. C. Sofotasios, I. Abualhaol, O. A. Dobre, and H. Yanikomeroglu, "Intelligent reflecting surfaces assisted UAV communications for IoT networks: Performance analysis," *IEEE Trans. Green Commun. Netw.*, vol. 5, no. 3, pp. 1029–1040, Sep. 2021.

[13] D. Ma, M. Ding, and M. Hassan, "Enhancing cellular communications for UAVs via intelligent reflective surface," in *Proc. IEEE Wireless Commun. Netw. Conf. (WCNC)*, May 2020, pp. 1–6.

[14] Z. Mohamed and S. Aïssa, "Leveraging UAVs with intelligent reflecting surfaces for energy-efficient communications with cell-edge users," in *Proc. IEEE Int. Conf. Commun. Workshops (ICC Workshops)*, Jun. 2020, pp. 1–6.

[15] M. Hua, L. Yang, Q. Wu, C. Pan, C. Li, and A. L. Swindlehurst, "UAV-assisted intelligent reflecting surface symbiotic radio system," *IEEE Trans. Wireless Commun.*, vol. 20, no. 9, pp. 5769–5785, Sep. 2021.

[16] S. Fang, G. Chen, and Y. Li, "Joint optimization for secure intelligent reflecting surface assisted UAV networks," *IEEE Wireless Commun. Lett.*, vol. 10, no. 2, pp. 276–280, Feb. 2021.

[17] L. Ge, P. Dong, H. Zhang, J.-B. Wang, and X. You, "Joint beamforming and trajectory optimization for intelligent reflecting surfaces-assisted UAV communications," *IEEE Access*, vol. 8, pp. 78702–78712, 2020.

[18] Z. Yao, W. Cheng, W. Zhang, and H. Zhang, "Resource allocation for 5G-UAV based emergency wireless communications," *IEEE J. Sel. Areas Commun.*, early access, Jun. 14, 2021, doi: 10.1109/JSAC.2021.3088684.

[19] D. V. Huynh, S. R. Khosravirad, L. D. Nguyen, and T. Q. Duong, "Multiple relay robots-assisted URLLC for industrial automation with deep neural networks," in *Proc. IEEE Global Commun. Conf. (GLOBECOM)*, Madrid, Spain, Dec. 2021, pp. 1–5.

[20] D. V. Huynh, S. R. Khosravirad, L. D. Nguyen, K. K. Nguyen, and T. Q. Duong, "Industrial IoTs clustering, joint blocklength and power optimisation for relay robots-aided URLLC in factory automation," *IEEE Internet Things J.*, under review.

[21] G. J. Sutton, J. Zeng, R. P. Liu, W. Ni, D. N. Nguyen, B. A. Jayawickrama, X. Huang, M. Abolhasan, Z. Zhang, E. Dutkiewicz, and T. Lv, "Enabling technologies for ultra-reliable and low latency communications: From PHY and MAC layer perspectives," *IEEE Commun. Surveys Tuts.*, vol. 21, no. 3, pp. 2488–2524, 3rd Quart., 2019.

[22] P. Yang, X. Xi, K. Guo, T. Q. S. Quek, J. Chen, and X. Cao, "Proactive UAV network slicing for URLLC and mobile broadband service multiplexing," *IEEE J. Sel. Areas Commun.*, vol. 39, no. 10, pp. 3225–3244, Oct. 2021.

[23] C. Pan, H. Ren, Y. Deng, M. Elkashlan, and A. Nallanathan, "Joint blocklength and location optimization for URLLC-enabled UAV relay systems," *IEEE Commun. Lett.*, vol. 23, no. 3, pp. 498–501, Mar. 2019.

[24] S. R. Sabuj, A. Ahmed, Y. Cho, K.-J. Lee, and H.-S. Jo, "Cognitive UAV-aided URLLC and mMTC services: Analyzing energy efficiency and latency," *IEEE Access*, vol. 9, pp. 5011–5027, 2021.

[25] S. Dimitrov and H. Haas, "Information rate of OFDM-based optical wireless communication systems with nonlinear distortion," *J. Lightw. Technol.*, vol. 31, no. 6, pp. 918–929, Mar. 15, 2013.

[26] A. Ranjha and G. Kaddoum, "URLLC facilitated by mobile UAV relay and RIS: A joint design of passive beamforming, blocklength, and UAV positioning," *IEEE Internet Things J.*, vol. 8, no. 6, pp. 4618–4627, Mar. 2021.

[27] Y. Polyanskiy, H. V. Poor, and S. Verdú, "Channel coding rate in the finite blocklength regime," *IEEE Trans. Inf. Theory*, vol. 56, no. 5, pp. 2307–2359, May 2010.

[28] R. I. Bor-Yaliniz, A. El-Keyi, and H. Yanikomeroglu, "Efficient 3-D placement of an aerial base station in next generation cellular networks," in *Proc. IEEE Int. Conf. Commun. (ICC)*, May 2016, pp. 1–5.

[29] Y. Pan, K. Wang, C. Pan, H. Zhu, and J. Wang, "UAV-assisted and intelligent reflecting surfaces-supported terahertz communications," 2020, *arXiv:2010.14223*. [Online]. Available: http://arxiv.org/abs/2010.14223

[30] W. Yang, G. Durisi, T. Koch, and Y. Polyanskiy, "Quasi-static multiple-antenna fading channels at finite blocklength," *IEEE Trans. Inf. Theory*, vol. 60, no. 7, pp. 4232–4265, Jun. 2014.

[31] Y. Gu, H. Chen, Y. Li, and B. Vucetic, "Ultra-reliable short-packet communications: Half-duplex or full-duplex relaying?" *IEEE Wireless Commun. Lett.*, vol. 7, no. 3, pp. 348–351, Jun. 2018.

[32] M. Alzenad, A. El-Keyi, and H. Yanikomeroglu, "3-D placement of an unmanned aerial vehicle base station for maximum coverage of users with different QoS requirements," *IEEE Wireless Commun. Lett.*, vol. 7, no. 1, pp. 38–41, Feb. 2018.

[33] T. Q. Duong, L. D. Nguyen, H. D. Tuan, and L. Hanzo, "Learning-aided realtime performance optimisation of cognitive UAV-assisted disaster communication," in *Proc. IEEE Global Commun. Conf. (GLOBECOM)*, Waikoloa, HI, USA, Dec. 2019, pp. 1–6.

[34] M.-H.-T. Nguyen, E. Garcia-Palacios, T. Do-Duy, L. D. Nguyen, S. T. Mai, and T. Q. Duong, "Spectrum-sharing UAV-assisted mission-critical communication: Learning-aided real-time optimisation," *IEEE Access*, vol. 9, pp. 11622–11632, 2021.

[35] A. Masaracchia, M. Nguyen, and A. Kortun, "User mobility into NOMA assisted communication: Analysis and a reinforcement learning with neural network based approach," *EAI Endorsed Trans. Ind. Netw. Intell. Syst.*, vol. 7, no. 25, Jan. 2021, Art. no. 167841.
[36] S. Diamond and S. Boyd, "CVXPY: A Python-embedded modeling language for convex optimization," *J. Mach. Learn. Res.*, vol. 17, no. 83, pp. 1–5, 2016.
[37] L. D. Nguyen, H. D. Tuan, T. Q. Duong, O. A. Dobre, and H. V. Poor, "Downlink beamforming for energy-efficient heterogeneous networks with massive MIMO and small cells," *IEEE Trans. Wireless Commun.*, vol. 17, no. 5, pp. 3386–3400, May 2018.
[38] A. A. Nasir, "Min-max decoding-error probability-based resource allocation for a URLLC system," *IEEE Commun. Lett.*, vol. 24, no. 12, pp. 2864–2867, Dec. 2020.
[39] H. Ren, C. Pan, Y. Deng, M. Elkashlan, and A. Nallanathan, "Joint power and blocklength optimization for URLLC in a factory automation scenario," *IEEE Trans. Wireless Commun.*, vol. 19, no. 3, pp. 1786–1801, Mar. 2020.

YIJIU LI received the bachelor's degree in automation from Shanghai University (SHU), China, in 2020. She is currently pursuing the Ph.D. degree with the School of Electronics Electrical Engineering and Computer Science, Queen's University Belfast, U.K. Her current research interests include ultra-reliable and low-latency communications (URLLC) with unmanned air vehicle (UAV), intelligent reflecting surface (IRS), and machine learning for real time optimization in wireless networks.

CHENG YIN received the Ph.D. degree in wireless communication from Queen's University Belfast (QUB), U.K., in 2019. She is currently a Research Fellow with the Centre for Wireless Innovation (CWI), QUB. Her research interests include machine learning, wireless communications, physical layer security, and green communication networking.

TAN DO-DUY received the B.S. degree from the Ho Chi Minh City University of Technology (HCMUT), Vietnam, in 2010, the M.S. degree from the Kumoh National Institute of Technology, South Korea, in 2013, and the Ph.D. degree from the Autonomous University of Barcelona, Spain, in 2019. He is currently with the Department of Computer and Communication Engineering, Ho Chi Minh City University of Technology and Education (HCMUTE), Vietnam, as an Assistant Professor. His main research interests include wireless cooperative communications, real-time optimization for resource allocation in wireless networks, and coding applications for wireless communications.

ANTONINO MASARACCHIA received the Ph.D. degree in electronics and telecommunications engineering from the University of Palermo, Italy, in 2016. His Ph.D. studies were conducted in joint supervision with the Institute of Informatics and Telematics (IIT), National Research Council (CNR), Pisa, Italy, and the obtained results have been important contributions from IIT to the FP7-MOTO European Project. Since 2018, he has been a Research Fellow with the Centre for Wireless Innovation, Queen's University Belfast, U.K. His research interests include fifth generation (5G) and beyond 5G networks, convex optimization and applied machine learning techniques to wireless communications, reconfigurable intelligent surfaces (RIS), UAV-enabled networks, and ultra-reliable and low-latency communications (URLLC). He was awarded with the Seal of Excellence delivered form the European Commission for his project submitted to Marie Skłodowska-Curie actions call H2020-MSCA-IF-2020. He is currently serving as a Guest Editor for *EAI Endorsed Transactions on Industrial Networks and Intelligent Systems* and a Special Issue on Radio Frequency Energy Harvesting and Wireless Power Transfer published by *Electronics* (MDPI), for which he serves also as a Topic Editor. He serves as a Guest Editor for a Special Issue on Controls, Communications and Networking for Ad-Hoc Mobile Sensor Networks published by *ICSES Transactions on Computer Networks and Communications*. He has served as a Guest Editor for a Special Issue on Reliable Communication for Emerging Wireless Networks published by *Mobile Networks and Applications* (ACM/Springer).

TRUNG Q. DUONG (Senior Member, IEEE) is currently a Chair Professor of telecommunications at Queen's University Belfast, U.K., and a Research Chair of the Royal Academy of Engineering. His current research interests include wireless communications, signal processing, machine learning, and data analytic with the applications in environment, disaster management, healthcare, agriculture, and industrial automation. He was awarded the Best Paper Award at the IEEE Vehicular Technology Conference (VTC-Spring), in 2013, the IEEE International Conference on Communications (ICC), in 2014, the IEEE Global Communications Conference (GLOBECOM), in 2016, the IEEE Digital Signal Processing Conference (DSP), in 2017, and GLOBECOM, in 2019. He was a recipient of prestigious Royal Academy of Engineering Research Fellowship (2015–2020) and has won a prestigious Newton Prize (2017). He currently serves as an Editor for the *Scientific Reports* (Nature), the IEEE TRANSACTIONS ON WIRELESS COMMUNICATIONS, and the IEEE TRANSACTIONS ON VEHICULAR TECHNOLOGY; and an Executive Editor for IEEE COMMUNICATIONS LETTERS.